# Mechanical spectra of glass-forming liquids. I. Low-frequency bulk and shear moduli of DC704 and 5-PPE measured by piezoceramic transducers

Hecksher, Tina; Olsen, Niels Boye; Nelson, Keith Adam; Dyre, J. C.; Christensen, Tage Emil

*Published in:*
Journal of Chemical Physics

*DOI:*
10.1063/1.4789946

*Publication date:*
2013

*Document Version*
Publisher's PDF, also known as Version of record

*Citation for published version (APA):*
Hecksher, T., Olsen, N. B., Nelson, K. A., Dyre, J. C., & Christensen, T. E. (2013). Mechanical spectra of glass-forming liquids. I. Low-frequency bulk and shear moduli of DC704 and 5-PPE measured by piezoceramic transducers. *Journal of Chemical Physics*, *138*(12A543), 12A543 1-12. https://doi.org/10.1063/1.4789946

# Mechanical spectra of glass-forming liquids. I. Low-frequency bulk and shear moduli of DC704 and 5-PPE measured by piezoceramic transducers

Tina Hecksher,[1,a)] Niels Boye Olsen,[1] Keith A. Nelson,[2] Jeppe C. Dyre,[1] and Tage Christensen[1]

[1]*DNRF Centre "Glass and time", IMFUFA, Department of Sciences, Roskilde University, Postbox 260, DK-4000 Roskilde, Denmark*

[2]*Department of Chemistry, Massachusetts Institute of Technology, Cambridge, Massachusetts 02139, USA*

(Received 12 November 2012; accepted 17 January 2013; published online 26 February 2013)

We present dynamic shear and bulk modulus measurements of supercooled tetraphenyl-tetramethyl-trisiloxane (DC704) and 5-phenyl-4-ether over a range of temperatures close to their glass transition. The data are analyzed and compared in terms of time-temperature superposition (TTS), the relaxation time, and the spectral shape parameters. We conclude that TTS is obeyed to a good approximation for both the bulk and shear moduli. The loss-peak shapes are nearly identical, while the shear modulus relaxes faster than the bulk modulus. The temperature dependence of this decoupling of time scales is constant over the temperature range explored here. In addition, we demonstrate how one can measure reliably the DC shear viscosity over ten orders of magnitude by using the two measuring techniques in combination. © *2013 American Institute of Physics*. [http://dx.doi.org/10.1063/1.4789946]

## I. INTRODUCTION

In contrast to solids, liquids cannot be clamped, bent, squeezed, pulled, or twisted. For this simple reason mechanical spectroscopy of liquids (viscous as well as non-viscous) presents a formidable challenge. Even highly viscous liquids close to the glass transition, which appear very solid-like, eventually flow on the time scale of the experiment, since we are usually interested in both the solid-like and the flow characteristics of the liquid. In one respect, though, liquids are simpler than crystalline solids: they are isotropic and thus under fixed thermal boundary conditions (isothermal or adiabatic) the number of independent elastic moduli reduces to two. This could be a combination of any two quantities like Young's modulus, Poisson's ratio, the shear modulus, the longitudinal modulus, or the bulk modulus. We choose here to regard as the two fundamental quantities the adiabatic bulk modulus (the pressure response to an adiabatic, shape-preserving deformation) and the shear modulus (the stress response to a volume-preserving deformation). Studies of such pairs of moduli are virtually nonexistent when the focus is on their frequency dependencies for highly viscous liquids.

In this first paper of a series on mechanical spectroscopy of glass-forming liquids, we present results from shear and (adiabatic) bulk modulus measurements carried out in the same experimental setup, i.e., the same cryostat and electronics, using methods first described in Refs. 1 and 2. The focus is on comparing the two mechanical response functions with respect to time scales, temperature dependencies, and spectral shapes. Also, we discuss how to determine as accurately as possible the absolute levels of the respective moduli, which is crucial when comparing to the other techniques as in Paper II.[3]

The background for comparing bulk and shear relaxations in viscous liquids is the following. Christensen and Olsen[4] compared the bulk and shear moduli of 1,2,6-hexanetriol. They concluded that the bulk relaxation was slower than the shear relaxation, while the spectral shapes were identical within the noise. Meng and Simon[5] presented pressure-relaxation measurements and compared the bulk results to shear creep compliance curves (measured by others) in polystyrene. They found that the bulk relaxation occurs in the short-time region of the shear response, contrary to the conclusion of Christensen and Olsen.[4] However, there may well be a difference between polymers and molecular liquids in this respect. Bulk and shear relaxations have been compared by several authors using (ultrasonic) measurements of longitudinal and shear sound waves.[6–10] Based on this procedure Marvin *et al.*[6] reported bulk and shear relaxation times as well as activation energies to be roughly equal. Morita *et al.*[7] found that the bulk relaxation was five times slower than shear relaxation, and Dexter and Matheson[8] reported a similar observation. Alig and co-workers[9–11] derived theoretically a relation between the bulk and shear viscosities (as defined below in Eqs. (3) and (6)) of polymers, $\eta^K/\eta^G = 2/3$, but found that the experiment ratio is larger than 2/3. Yee and Takemori[12] developed a method by which Young's modulus and Poisson's ratio could be measured simultaneously on a sample. Combining the measured quantities they were able to calculate the bulk and shear moduli, and their results suggested that the time scale for relaxation is very similar. Of these studies only some compared response functions measured in the same experimental setups (Refs. 1, 7, and 12).

This paper is structured as follows: In Sec. II, we give some experimental details of the measurements, while more technical details are given in Appendices A and B. Sections III A and III B present the data and characterize these in terms of time-temperature superposition (TTS), time scales

a)Electronic mail: tihe@ruc.dk.

 

of the alpha relaxation, and spectral shapes. This is followed by Sec. IV in which the consistency between data for the DC shear viscosity obtained in two independent ways from the two measuring techniques is established. The conclusions are summarized briefly in Sec. V.

## II. EXPERIMENTAL DETAILS

Measurements were performed on two commercial diffusion-pump oils: tetramethyl-tetraphenyl-trisiloxane (DC704) and 5-phenyl-4-ether (5-PPE). Both stem from old bottles (>10 years) but have proven to be extremely stable and give reproducible results over the entire lifetime of the bottle. These liquids were chosen because they have a number of convenient properties: they are not prone to crystallize which is important as crystallization may break our measuring cells, their $T_g$'s are in the working range of our cryostats, they are easy to handle at room temperature, and they are chemically stable and non-toxic. The liquids were used as purchased from Sigma-Aldrich and Santovac Inc., respectively, and used with no further purification. The glass transition temperature, $T_g$, of DC704 is 210 K and $T_g$ of 5-PPE is 245 K. Both liquids are rather fragile with Angell fragility index of $m \simeq 80$.

The general experimental setup and the cryostat have been described in details by Igarashi *et al.*[13,14] All measurements were carried out in the same closed-cycle cryostat. This procedure ensures that all measurements are performed under close-to-identical experimental conditions. The temperature stability of the cryostat is better than 10 mK, and the absolute temperature calibration is better than 0.1 K.

The Piezo-electric Bulk modulus Gauge (PBG) and the Piezo-electric Shear modulus Gauge (PSG) techniques were developed some time ago,[1,2] but are still undergoing improvements. Both techniques rely on the piezo-electric effect, i.e., the coupling between the electric field and the strain state of the piezo-electric material, and both methods have a large dynamical range spanning from approximately 1 mHz to 10 kHz. The upper limit is set by the first resonance, which for both transducers lies around 100 kHz.

Below we give a brief description of the working principles of these devices. Appendix A gives a more detailed description of the PSG, while Appendix B gives some specific details on the PBG technique. For full descriptions we refer to Christensen and Olsen[1,2] and Hecksher.[15]

The PSG[2] is a layered construction of three piezo-electric ceramic discs (see Fig. 1). When subjected to an electrical field the discs expand or contract in the radial direction. The three discs are electrically connected such that the middle disc moves opposite the two outer discs. The liquid is loaded in the two gaps between the discs. Consequently, an electric field results in a shear deformation of the liquid layers. A "stiff" (viscous) liquid partially clamps the discs, causing a drop in the measured capacitance compared to that of the empty device. This capacitance drop is mathematically related to the shear modulus of the liquid.[2]

The PBG[1] consists of a piezo-electric ceramic shell with electrodes on the inside and the outside (Fig. 1). The ceramic is polarized in the radial direction. Consequently, when a voltage is applied to the electrodes, the ceramic deforms in the radial direction, increasing or decreasing the inner volume of the shell depending on the direction of the field. A liquid inside the shell partially clamps the shell and thus changes the capacitance of the shell compared to that of a freely moving shell. The difference in capacitance of the shell between empty and liquid-filled shells is mathematically related to the bulk modulus of the liquid.[1] In the available frequency region, the PBG measures the adiabatic rather than the isothermal bulk modulus. This is the case whenever the heat diffusion length $l_D = |\sqrt{D/i\omega}|$ is much smaller than the radius of the ceramic sphere, $R = 9$ mm. Here, $D$ is the diffusion constant and $\omega$ the angular frequency. In our frequency range we have $2.8 \text{ mm} < l_D < 0.001$ mm. Thus, the isothermal limit is approached at the lowest frequencies, but here even the adiabatic criterion $l_D \ll R$ applies to a good approximation.

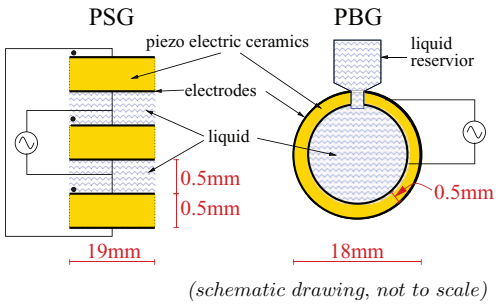


FIG. 1. Schematic drawings of the Piezo-electric Shear modulus Gauge (PSG) and the Piezo-electric Bulk modulus Gauge (PBG). The blue wavy lines represent the liquid. The PSG consists of three piezo-electric discs in a layered construction, all polarized in the $z$-direction (the polarization direction is marked by a small dot). The discs are electrically connected as shown, which results in the field direction in the middle disc always being opposite the two outer discs. Consequently, the middle disc moves opposite the outer discs, creating a shear deformation of the two liquid layers between the discs. The PBG consists of a piezo-electric shell with electrodes inside and outside. When an electrical field is applied, the shell deforms, creating a larger or smaller inner volume, thus enforcing a volume deformation on the liquid inside the shell. The device is filled through a small hole in the ceramic shell. To allow for thermal contraction of the liquid, a reservoir is attached over this hole, thus ensuring that the liquid is filling the full volume of the shell at all temperatures. For more details, see Refs. 1 and 2.

The liquid is loaded through a small hole in the shell. This hole must be kept open because the liquid contracts upon cooling and the PBG needs to draw in extra liquid in order to fill the volume. The existence of the hole limits the temperature (or rather the relaxation time) range of the measurement. The time it takes for the liquid to flow in through the hole is proportional to the shear viscosity, and this time gets very large when the glass transition temperature is approached. As demonstrated below, the hole allows for an independent measurement of the DC shear viscosity compared to that derived directly from a dynamic shear modulus measurement, because the hole flow may be modelled as a Poiseuille flow.

A complication of these methods is that the properties of piezo-electric ceramic material are both temperature dependent and dependent on thermal history. The bulk/shear modulus is extracted from the measurement of difference in the capacitance of the empty device and of the filled device; this means that for each measurement the temperature protocol needs to be repeated with the empty device in order to

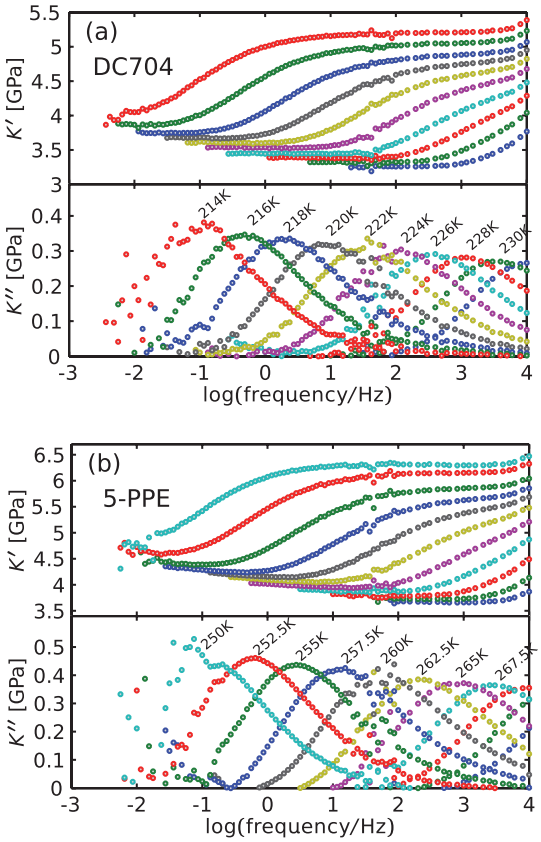


FIG. 2. Bulk modulus data of DC704 and 5-PPE. (a) Real and imaginary parts of the bulk modulus for DC704 from 214 K in steps of 2 K up to 232 K. (b) Real and imaginary parts of the bulk modulus for 5-PPE from 250 K in steps of 2.5 K up to 275 K.

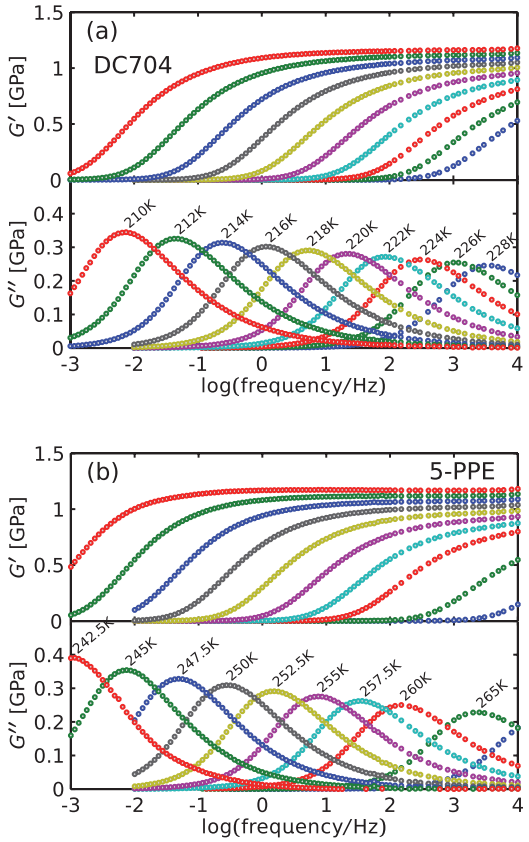


FIG. 3. Shear modulus data of DC704 and 5-PPE. (a) Real and imaginary parts of the shear modulus of DC704 from 210 K in steps of 2 K up to 228 K. (b) Real and imaginary parts of the shear modulus of 5-PPE from 242.5 K in steps of 2.5 K up to 260 K, and at 265 K and 270 K.

ensure identical thermal histories. We refer to these as the liquid measurement and the reference measurement.[35]

## III. DATA AND THEIR CHARACTERIZATION

Figure 2 shows the real and imaginary parts of the complex bulk moduli of DC704 and 5-PPE, while the complex shear moduli are shown in Fig. 3. The characteristic viscoelastic behavior of supercooled liquids is evident: At low frequencies (corresponding to long times) the behavior is liquid-like; for the shear modulus this means that the real part vanishes as frequency goes to zero, while the bulk modulus at low frequencies converges to constant finite (low) value, $K_0$. At high frequencies the behavior is solid-like, which for both bulk and shear moduli implies a (higher) plateau value of the real part. For both DC704 and 5-PPE, the high-frequency level of the bulk modulus ($K_\infty$) is roughly five times higher than the high-frequency level of the shear modulus ($G_\infty$).

In between these limits there is a transition from liquid- to solid-like behavior. This gives peaks in the imaginary parts of the moduli that identify the characteristic frequency (time scale) of the liquid. This characteristic time scale is strongly temperature dependent close to the glass transition, as is evident from Figs. 2 and 3 where this transition shifts six orders of magnitude over a 20 K temperature interval.

The bulk modulus data of DC704 cover temperatures from 214 K to 232 K in steps of 2 K, the corresponding shear modulus data go down to 210 K. The temperature interval for the bulk modulus of 5-PPE is from 250 K to 275 K in steps of 2.5 K, and for the shear modulus from 242.5 K to 260 K (same step size) as well as 265 K and 270 K. The temperature range of the bulk modulus measurement is limited due to the slow flow in and out of the reservoir as described in Sec. II.

Bulk modulus data of these liquids have not been published before, while the shear modulus was measured previously by Jakobsen *et al.*[16] The agreement between their set of measurements and the present is excellent with respect to relaxation shapes and relaxation times, although there are up to 40% deviations on the absolute levels of $G_\infty$. This discrepancy can be due to imperfect filling of the PSG or imperfect match of liquid and reference measurement. We believe that the present measurements have relatively small error bars on absolute levels because of the excellent agreement between the shear viscosity measured by the PSG and PBG (see Sec. IV below).

### A. Time-temperature superposition

Time-temperature superposition refers to the property that the shape of a given relaxation function is unchanged when the temperature is varied and only the position on the logarithmic time/frequency axis shifts. In mechanical measurements, TTS is often assumed in order to construct a master curve spanning more decades of frequency than the

time/frequency window of the actual measurement. Based on dielectric measurements, which usually have quite a large frequency span, it has been suggested that TTS applies for the main (alpha) relaxation whenever it is not influenced by other processes.[17] Wang and Richert[18] observed a progressive narrowing of the relaxation at temperatures much above the glass transition, while Nielsen *et al.*[19] reported both broadening and narrowing of the dielectric relaxation with temperature close to the glass transition in a comparative study of a large number of liquids. With the relatively large frequency span of our techniques, we can test whether TTS applies.

A standard way of checking for TTS in frequency-domain data is to make a dimensionless plot of the imaginary part of the response function (the "loss"), i.e., scaling the frequency axis with the peak position and the *y*-axis by the peak height ($\omega/\omega_{\max}$, $\chi''/\chi''_{\max}$), where $\chi$ represents the complex response function. If this scaling makes the data collapse, TTS is obeyed. Normally this is a qualitative statement. A quantitative TTS measure was recently proposed and applied to dielectric data by Nielsen *et al.*,[19] a method that requires extremely low-noise data and unfortunately cannot be used to characterize our mechanical data.

Another, less commonly used, way of checking for TTS is via a normalized Cole-Cole (Nyquist) plot. A Cole-Cole plot is constructed by plotting the complex response function as ($\chi'(\omega)$, $\chi''(\omega)$) parametrized via the (angular) frequency $\omega$. Defining the normalized relaxation function, $F(\omega) = (\chi(\omega) - \chi_0)/(\chi_\infty - \chi_0)$, the normalized Cole-Cole plot is defined by ($F'(\omega)$, $F''(\omega)$). The advantage of using a normalized Cole-Cole plot is that it includes both the real and imaginary parts and thus is a more complete representation of the data than merely plotting the imaginary part as a function of frequency. Also, in Cole-Cole plots the entire data set from $\omega \to 0$ to $\omega \to \infty$ is contained in a single plot. In this representation a Debye process traces out a semi-circle with radius 1/2 and center on the real axis. The typical alpha process, on the other hand, is more flat and skewed to the high-frequency side.

In Fig. 4, we show both types of TTS plots for the shear and bulk relaxations of DC704 and 5-PPE. Within the noise, TTS is obeyed for the bulk modulus of both DC704 and 5-PPE. In the less noisy shear modulus data, it is seen that while the DC704 shows near perfect data collapse, the 5-PPE data have small deviations on the high-frequency side of the alpha relaxation peak. There is a temperature-dependent high-frequency wing in the spectrum, which could be due to a small-amplitude beta process according to the conjecture of Olsen *et al.*[17]

Both bulk and shear relaxation shapes for DC704 and 5-PPE are quite similar. In the shear data we do see a small difference between the two substances: 5-PPE is a bit narrower than the DC704, which in the Cole-Cole representation corresponds to a slightly higher peak position. In Fig. 5, we combine the TTS curves of bulk and shear modulus relaxation (bulk data in (black) empty circles and shear data in (cyan) dots). For DC704 the less noisy shear-modulus data trace out a curve that the bulk modulus data are scattered around. For the 5-PPE data there are slight deviations from this picture. In the loss peak, TTS scaling the bulk modulus peak is a little broader than the shear modulus peak. This shows up as

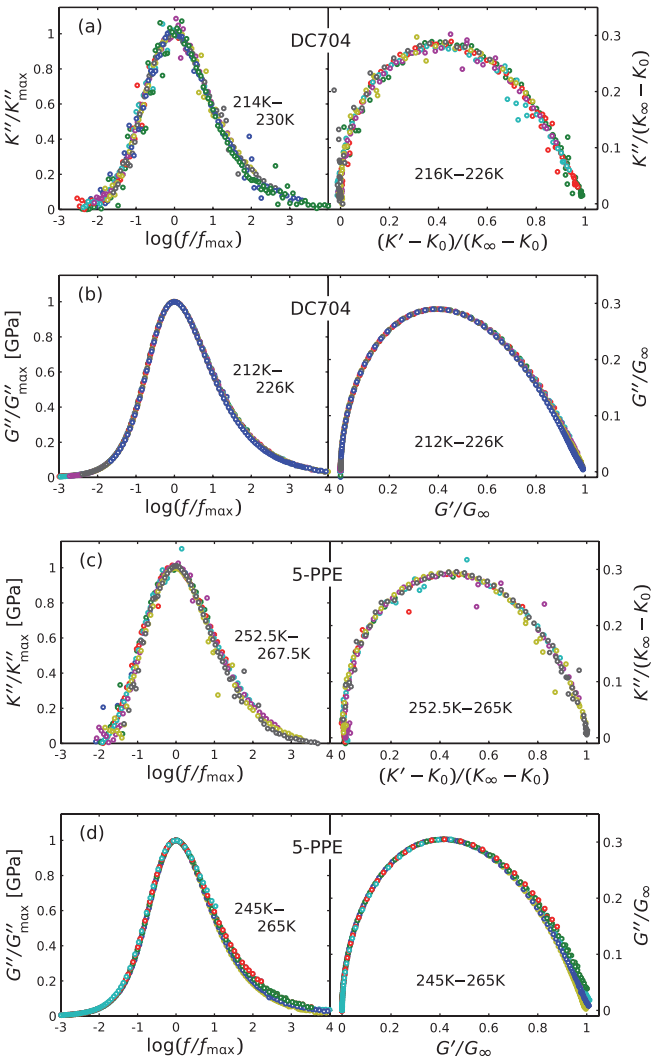


FIG. 4. TTS plots of the bulk and shear modulus. (a) Bulk modulus of DC704, (b) shear modulus of DC704, (c) bulk modulus of 5-PPE, and (d) shear modulus of 5-PPE. The bulk modulus data are more noisy than the shear data, but within the noise TTS is obeyed for the bulk modulus of both DC704 and 5-PPE. With less noise in the shear modulus spectra, an indication of a small wing is seen in 5-PPE. Thus, 5-PPE does not obey TTS perfectly although the deviation is very small, while TTS is nearly perfectly obeyed in the shear data for DC704.

a slighter flatter shape in the Cole-Cole representation. This may be an artifact stemming from an imperfect match between liquid and reference scan. The odd shape on the low-frequency side of the peak (the curve goes below zero instead of flattening out) supports this. Similarity between the bulk and shear relaxations was noted previously by Morita *et al.*[7] (in a polymer) and by Christensen and Olsen[1] (for the alcohol 1,2,6-hexanetriol).

A low frequency cutoff of the bulk modulus data presented in Fig. 2(a) was introduced to get rid of the signal due to liquid flowing in and out of the piezo-ceramic shell at low frequencies, since this feature is unrelated to the bulk modulus relaxation. This phenomenon is known in the literature as an over-damped Helmholtz resonator, and as mentioned in Sec. II the position of this mode is determined by the shear viscosity. Including this feature in the TTS plot thus illuminates the relation between shear and bulk viscosities.

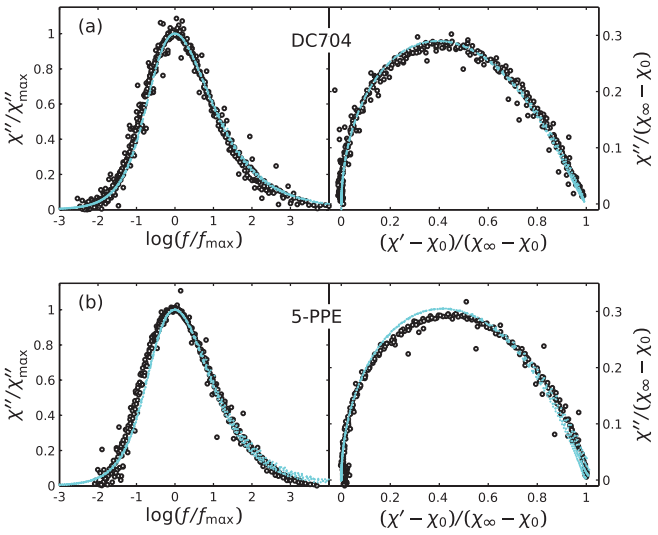


FIG. 5. Same plots as in Fig. 4, but now with the bulk and shear data plotted together for (a) DC704 and (b) 5-PPE. The bulk data are given in black symbols, the shear data in blue symbols. It appears that the shape of the bulk and shear relaxation is the same, most convincingly for DC704.

Consequently, we scaled the bulk modulus curves to the peak position of the Helmholtz mode (Figure 6). In order to do so, the peak must be in the frequency window of the measurement, which limits the range of temperatures that can be included in the analysis to the higher temperatures.

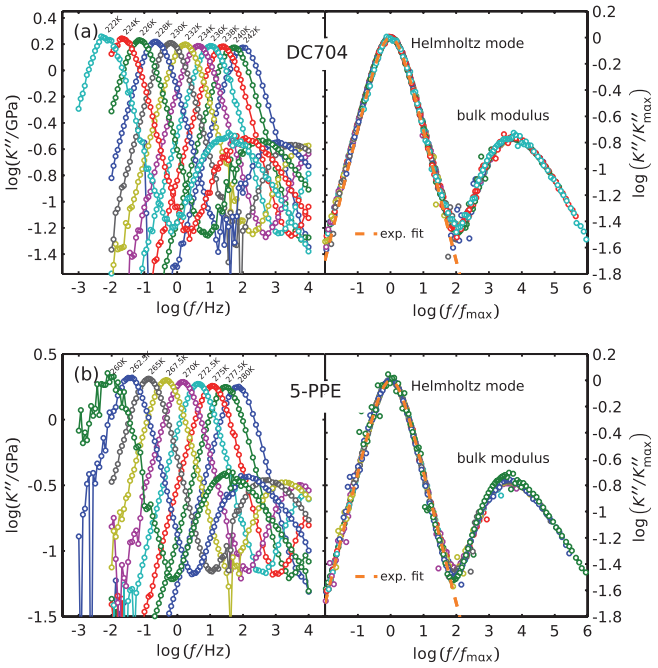


FIG. 6. Full signal from the bulk modulus measurement including the Helmholtz mode (see text) of the liquid flowing in and out of the reservoir for (a) DC704 and (b) 5-PPE. The left panels show the imaginary parts of the signals as functions of frequency at different temperatures. The right panels show the same spectra scaled to the position of the Helmholtz mode. For DC704, TTS is clearly obeyed over the entire region, while 5-PPE shows small deviations from this at the lowest temperatures. The orange dashed line is a pure Debye curve, confirming the exponential nature of the Helmholtz mode (see Appendix C).

Figure 6 shows the imaginary part of the bulk modulus as a function of frequency, also including the Helmholtz mode of the liquid flowing in and out of the hole, as well as these curves scaled with the peak position of the Helmholtz mode. Being exponential in nature, the Helmholtz mode obviously scales, but perhaps more surprising is the fact that this procedure simultaneously scales the bulk modulus: The entire signal collapses into a single curve. For DC704, the collapse is close to perfect; both the minimum between the two peaks and the height and position of the bulk modulus relaxation collapse. For 5-PPE, the minimum decreases slightly and the maximum of the bulk modulus relaxation increases with decreasing temperature, slightly destroying the data collapse. The peak position of the bulk relaxation relative to the Helmholtz mode; however, seems to be unchanged.

Time-temperature superposition for the entire curve suggests that the bulk and shear viscosities are proportional in the temperature range included here. We next look into the question of the relation between the bulk and shear relaxation time scales.

## B. Loss-peak frequencies and shape parameters

For a given response, the relaxation time $\tau$ may be defined in different ways. It may be defined as the fitting parameter $\tau$ of various fitting functions such as the stretched exponential (KWW) function $\varphi = \varphi_0 \exp(-(t/\tau)^\beta)$ in the time-domain or the Havrilak-Negami function $\chi = \chi_\infty + \Delta\chi/(1 + (i\omega\tau)^\beta)^\alpha$ in the frequency domain. Alternatively, $\tau$ may be identified from model-free definitions, for instance, the integral $\tau = \int_0^\infty \varphi(t)/\varphi_0\, dt$ or the inverse of the angular loss-peak frequency. For exponential relaxations, all these definitions give the same $\tau$'s. For non-exponential relaxations the $\tau$'s are proportional (as functions of temperature) if TTS is obeyed.

Probably the most robust and convenient model-free method to determine the time scale of a relaxation process is determining the loss-peak frequency, $f_{max}$, and for all measurements presented here this is indeed possible. The peak position is determined by fitting a second-order polynomial to a number of points around maximum of the loss.[19] The number of data points we included in the fit depended on the noise. For the shear modulus relaxation, a total of five points were sufficient. For the lowest temperature of the bulk modulus data we included up to 15 points. The results are shown in Fig. 7(a) where the full symbols give the 5-PPE data and the open symbols the DC704 data. In both cases the shear modulus relaxes faster than the bulk modulus. This agrees with the conclusion of Christensen and Olsen[1] and Morita *et al.*[7]

Time scales of different probes are sometimes[16,20–22] compared through the so-called time-scale index $X$ defined by

$$X(\chi_1, \chi_2, T) = \frac{\tau_{\chi_1}(T)}{\tau_{\chi_2}(T)}. \quad (1)$$

Here the $\chi$'s are two different probes, $\tau_\chi$'s are the time scale of that particular probe, and $T$ is the temperature. If $X$ is constant we define the time scales of the two probes to be coupled. Figure 7(b) shows the logarithm of the time scale index of the bulk and shear relaxations. The shear modulus relaxes

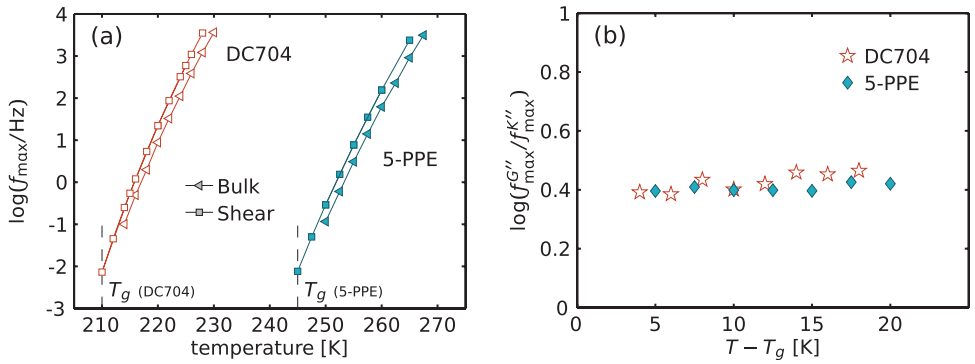


FIG. 7. (a) Loss-peak frequencies for the bulk and shear relaxations. (Symbols) Bulk modulus (triangles), shear modulus (triangles), loss-peak frequencies of DC704 (open symbols), and 5-PPE (full symbols). (b) Time-scale index (see Eq. (1)) for the bulk and shear relaxations. The shear modulus relaxes roughly 0.4 decades (equivalent to 2.5 times) faster than the bulk modulus in both DC704 and 5-PPE.

roughly 0.4 decades (2.5 times) faster than the bulk modulus at all temperatures, and the bulk and shear relaxation times are clearly coupled.

There is no clear trend in previous works regarding the temperature dependence of $X$, which apparently depends both on the liquid under investigation and the probes used. There are reports of constant time-scale indices in measurements,[23–26] as well as reports of a temperature-dependent time scale indices.[27–29] Sometimes the relaxation times (or peak frequencies) of different probes are simply compared in an Arrhenius plot ($\log\tau$ or $\log\omega_{\max}$ as a function of inverse temperature) of different probes without explicitly evaluating the time scale index, see, e.g., Schröter and Donth,[30] who collected data on glycerol from dielectric, heat capacity, shear retardation, and nuclear magnetic resonance measurements. However, none of these studies compare quantities measured under identical experimental conditions, which is critical when comparing, e.g., relaxation times which are extremely temperature dependent. Even small deviations ($<1\%$) in the temperature calibration can give rise to spurious decoupling.

We prefer to characterize the shape of the relaxation function in terms of the model-independent parameters: minimum slope[17] and normalized half width.[31] The minimum slope is defined as the minimum of the logarithmic derivative of the high-frequency part of spectrum

$$\alpha_{\min} = \min_{f>f_{\max}} \left( \frac{d\log\chi''}{d\log f} \right), \tag{2}$$

which is a negative number giving the high-frequency approximate power-law decay. Since the low-frequency side of the loss peaks of viscous liquids is usually Debye like, $\alpha_{\min}$ is a measure of the stretching of the relaxation function. This is similar to the well-known model parameters $\beta_{SE}$ and $\beta_{CD}$ of the stretched exponential function and the Cole-Davidson fitting functions, respectively. Determining the minimum slope involves taking the numerical derivative of the data, and this only works well for low-noise measurements. For most dielectric data this is an excellent method to characterize the spectral shapes of relaxation as documented by Nielsen *et al.*[19] For shear relaxation data it works reasonably well, while the bulk modulus data are too noisy for this procedure. Alternatively, one may use the quantity $W$ defined as the width of the loss spectrum at half maximum. It is straightforward to determine $W$, and we have been able to do so even for the bulk spectra.

We show the shear relaxation minimum slopes of DC704 and 5-PPE as functions of loss-peak frequencies in Fig. 8(a) compared to the values obtained in 2005 by Jakobsen *et al.*[16] for the same substances (in smaller symbols). There is a good agreement between the data sets.

Figure 8(b) reports the widths normalized to the width of a Debye process, $W/W_D$, for both bulk and shear data. The scatter is quite large for the bulk relaxation values, which reflects the relatively large noise in the measurement itself. Within the scatter, bulk and shear measurements agree, which is also what is expected based on the TTS analysis presented in Fig. 5. The width of the DC704 shear relaxation decreases slightly from $-0.42$ to $-0.46$ with decreasing temperature, while the 5-PPE values decrease from roughly $-0.40$ to $-0.55$. This again confirms that TTS is well obeyed in DC704, whereas there are minor deviations from TTS in 5-PPE.

Both width and minimum slope for DC704 agree very well with previous results, while we observe a discrepancy between widths of the shear relaxation in the present measurements and the values reported in Ref. 16 for 5-PPE. The latter are shifted towards lower values (narrower spectral shape), but the loss-peak frequency dependence (or, equivalently, the temperature dependence) is similar. Jakobsen and Niss[32] showed that imperfect filling of the shear transducer can lead to a spurious broadening of the spectral shape, which presumably explains the discrepancy.

## IV. VISCOSITY DETERMINED THROUGH BULK AND SHEAR MODULI

We can determine the DC shear viscosity from the measurement of the shear modulus. Recall that the complex shear viscosity is defined as[33]

$$\eta_G(\omega) = \frac{G(\omega)}{i\omega}. \tag{3}$$

This means that the DC shear viscosity is given by

$$\eta_G^{DC} = \eta_G'(\omega \to 0) = \lim_{\omega\to 0} \frac{G''(\omega)}{\omega}. \tag{4}$$

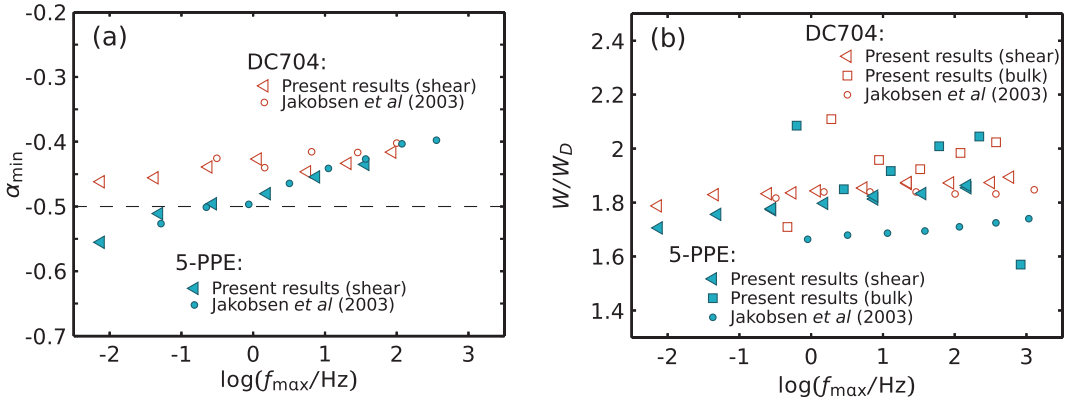


FIG. 8. Spectral shape parameters for DC704 and 5-PPE. (a) The minimum slope (Eq. (2)) is a measure of how stretched the relaxation is. Large symbols are from present measurements, small symbols give the parameters reported by Jakobsen *et al.*[16] Bulk modulus relaxation data were too noisy to extract any meaningful minimum slope value. There is excellent agreement between the present results and previously reported[16] values. (b) Full width at half maximum of the loss peak normalized to the width of a Debye process. Again, shear relaxation values are compared to previously reported data by Jakobsen *et al.*[16] In the case of DC704 there is a good agreement between the two data sets. For 5-PPE there is a small discrepancy in absolute numbers, but not in temperature dependence. Thus, both width and minimum slope varies weakly with temperature for DC704 and slightly more in the case of 5-PPE. This is consistent with the small deviations found in the TTS plots in Fig. 4.

The DC shear viscosity is roughly proportional to the relaxation time according to the Maxwell relation $\tau = \eta_G^{DC}/G_\infty$,[33] since the temperature dependence of $G_\infty$ is small compared to that of the shear viscosity.

In Figs. 9(a) and 9(b), we show the real part of the viscosity $\eta_G' = G''(\omega)/\omega$ as a function of frequency for the two liquids. Approaching frequencies that are low compared to the inverse alpha relaxation time, the curves bend over and settle at a plateau. The DC shear viscosity was identified from the lowest frequency data point of these curves. For the lowest temperature of DC704 and the two lowest temperatures of 5-PPE, we do not really observe the plateau, and this procedure thus underestimates the DC shear viscosity at the lowest temperatures. To circumvent this problem, we shifted one of the curves with a clear plateau value with the relative loss-peak position. Since TTS holds to a good approximation in both DC704 and 5-PPE, this is a valid procedure. These curves are shown as grey lines and the plateau of these curves gives a better estimate of the DC shear viscosity at the lowest temperatures.

We can also infer the DC shear viscosity from the bulk modulus measurements. At low frequencies the liquid flows in and out of the hole in the piezo-ceramic shell, and this Poiseuille flow is governed by the shear viscosity of the liquid.[1] Thus, if the dimension of this "tube" is known, one is able to determine the shear viscosity from the Helmholtz mode in the bulk modulus measurements.

Equation (C2) of Appendix C shows that the shear viscosity is proportional to the mechanical flow resistance, $R_P$ (defined below),

$$\eta_G^{DC} = AR_P, \tag{5}$$

where $A = \pi a^4/8l$ is geometric factor, $a$ and $l$ being the radius and length of the tube, respectively. The dimensions of this tube were measured to be $a = 0.9$ mm and $l = 3.75$ mm. This gives $A = 6.9 \times 10^{-11}\text{m}^3$, which is the value used. But even if we did not know the specifications, the geometric factor is a number specific to a given measuring cell, which can be calibrated with a single set of measurements. A Poiseuille flow

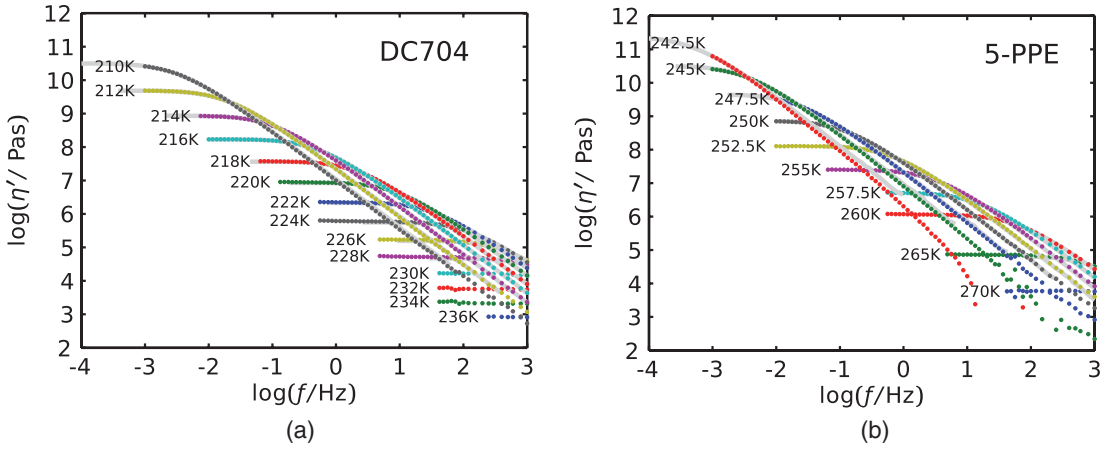


FIG. 9. Determining the shear viscosity from shear modulus measurements for (a) DC704 and (b) 5-PPE. The figures show $\eta' = G''/\omega$ plotted against frequency. Clearly, this quantity approaches a constant value for $\omega \to 0$, which identifies the static shear viscosity.

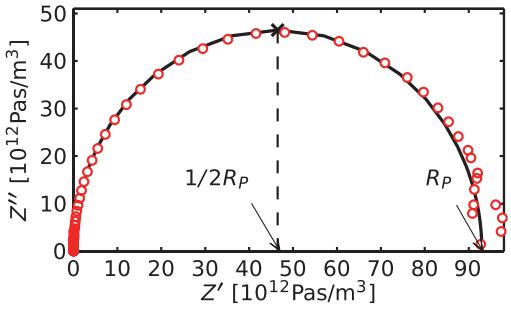


FIG. 10. Determining the flow resistance $R_P$ from an impedance Cole-Cole plot of the Helmholtz mode data of the PBG. The mechanical impedance of DC704 at 232 K is shown in red symbols, the black solid line shows an exponential fit, and the arrows show how $R_P$ can be determined (see also Fig. 18 in Appendix C). The data at the right foot point reflect the relatively large noise in the measurement at low frequencies.

normally requires $a \ll l$, which may not be the case here, but it turns out to be a good approximation.

$R_P$ as a function of temperature is determined through the mechanical impedance, $Z = S/i\omega$, where $S = \delta p/\delta V$ is the stiffness found in the bulk modulus measurement (Eq. (B7)). $R_P$ is identified as the low-frequency foot point of the Cole-Cole representation of the mechanical impedance from the peak position, $Z''_{\max} = 1/2R_P$. This is illustrated in Fig. 10 where the mechanical impedances of DC704 at 234 K are shown. Data points are (red) dots and an exponential fit is shown as a solid line. Identifying the peak position requires the peak to be in the measured frequency window; thus this method is restricted to relatively high temperatures.

The shear viscosities determined from these two methods are compared in Fig. 11. For both liquids the viscosities as measured by these two methods match up perfectly. This is the case, despite the fact that boundary effects could well give rise to a correction term to the Poiseuille formula, which refers to flow in an infinitely long tube. The two fundamentally different measuring methods thus confirm the absolute levels of the shear and bulk moduli, since these influence the determined values of the viscosity. Consequently, combining the shear and bulk modulus measurements we are able to measure reliably both moduli for a wide dynamical range. In particular, the bulk and shear modulus measurements in combination provide a novel and accurate way of measuring the shear viscosity over ten orders of magnitude.

The bulk viscosity is defined in analogy to the shear viscosity from,

$$\eta_K(\omega) = \frac{K(\omega)}{i\omega}. \tag{6}$$

In principle, we should be able to determine the DC limit analogous to Eq. (4), $\eta_K^{DC} = \lim_{\omega\to 0} K''/\omega$. In Fig. 12, the low-frequency limit of the bulk viscosity is shown as colored circles and the shear viscosity as black lines. The bulk viscosity curves are quite noisy, though, and the procedure of taking the last data point for each temperature as the DC limit would result in very noisy data. To extract a meaningful number from these curves a more advanced approach or some modelling is needed, which we have not yet done. But the same trend as for the shear viscosity is observed, namely, that the bulk viscosity bends over to form a plateau at low frequencies, which also means that the pressure relaxation is exponential at long times (low frequencies).

Interestingly, the bulk and shear viscosity curves collapse *but not for the same temperatures*. For instance, the bulk viscosity curve for 220 K for DC704 falls on top of the shear viscosity curve for 218 K. The trend is the same for 5-PPE: the bulk and shear viscosity curves are similar, but at different temperatures. We conclude that the bulk and shear viscosities are very similar, though not identical, the bulk viscosity being higher than the shear viscosity at a given temperature. This is in accord with the decoupling between the time scales of the bulk and shear relaxations found earlier, assuming a correspondence between bulk viscosity and bulk modulus relaxation time similar to the Maxwell relation for shear. The bulk viscosity is higher than the shear viscosity at all measured temperatures, just as the bulk relaxation time is longer than the shear relaxation time. Unfortunately, the bulk viscosity data are not good enough for a more quantitative statement.

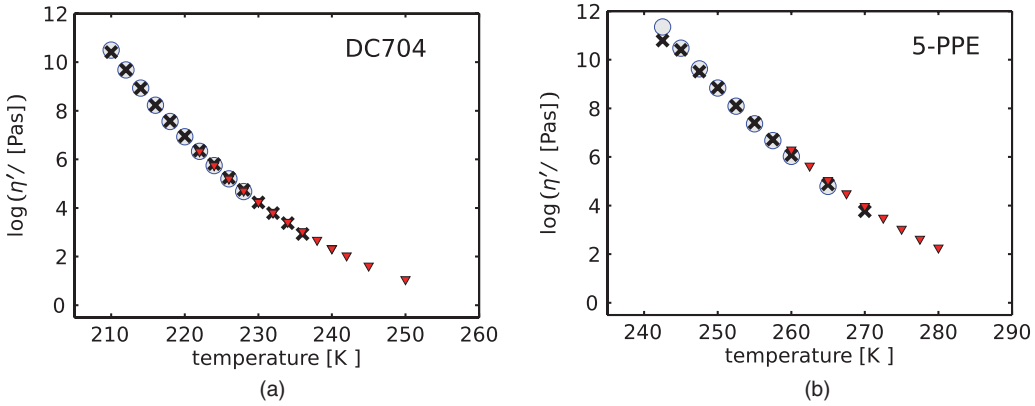


FIG. 11. Comparing the shear viscosities obtained by two different methods for (a) DC704 and (b) 5-PPE. Circles are determined from the low-frequency limit of the shear modulus (Eq. (4)) using TTS extrapolation, crosses are the lowest frequency points of the curves in Fig. 9, and full triangles are determined by analyzing the Helmholtz mode data at low frequencies of the bulk modulus measurement. The agreement between the different methods is excellent. The figure demonstrates a novel and accurate way to determine the shear viscosity over many decades.

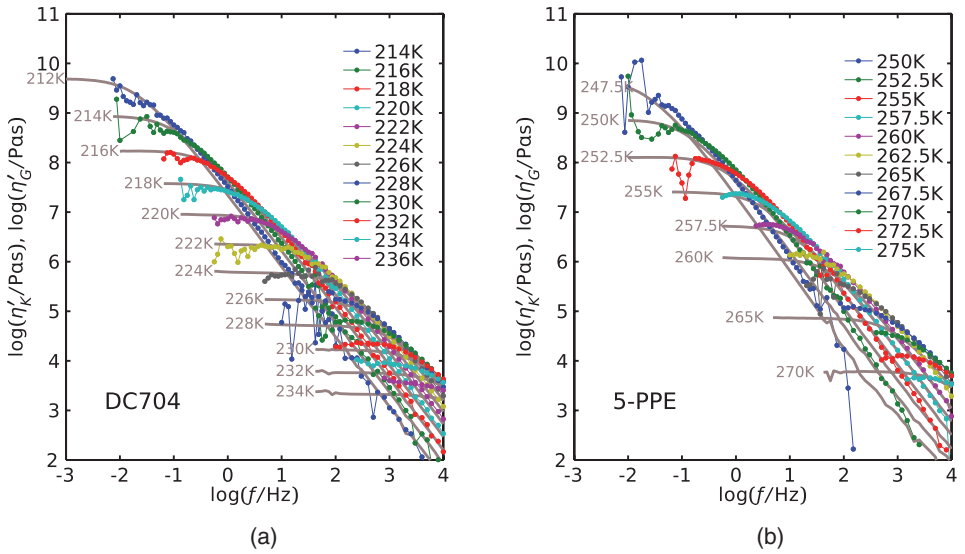


FIG. 12. Determining the bulk viscosity from bulk modulus measurements for (a) DC704 and (b) 5-PPE. The figures show $\log(K''/\omega)$ plotted against frequency. This quantity approaches a constant value for $\omega \to 0$, as was the case for the shear viscosity. For comparison we also plotted the shear viscosity curves (grey lines). For DC704, the bulk and shear viscosity curves more or less collapse, but at different temperatures. 5-PPE shows the same pattern although with lower quality of the bulk viscosity curves.

## V. SUMMARY

Based on the above we conclude the following:

- TTS is obeyed for both shear and bulk moduli in DC704, whereas small deviations are seen for 5-PPE.
- There are no clear signs of any $\beta$ relaxation in DC704 or 5-PPE, but the small deviations from TTS in 5-PPE may be a signature of a small-amplitude $\beta$ process.
- The bulk and shear modulus relaxation shapes are nearly identical for DC704 and 5-PPE.
- The time scales of bulk and shear relaxations are different, but proportional in the measured temperature range explored.
- The (DC) bulk viscosity is larger than the (DC) shear viscosity at a given temperature.
- Shear viscosities as determined by $\eta = \lim_{\omega \to 0} G''/i\omega$ and as determined by the Poiseuille flow in the PBG hole agree, showing that absolute levels of the shear modulus and bulk modulus are mutually consistent.

DC704 and 5-PPE thus show simple patterns of mechanical relaxation. It would be interesting to investigate how general these findings are.

## ACKNOWLEDGMENTS

The centre for viscous liquid dynamics "Glass and Time" is sponsored by the Danish National Research Foundation's Grant No. DNRF61.

## APPENDIX A: MODELING THE PSG

The PSG consists of three electrode-covered piezo-electric ceramic discs mounted in a layered construction, which prevents unwanted bending of the discs and further has the advantage that it can be mapped mathematically to a one-disc system involving a fixed wall.[2]

The liquid is loaded into the 0.5 mm gaps between the discs (Fig. 1). Depending on the polarity of the discs compared with the direction of an applied electric field, the discs expand or contract in the radial direction. Electrically, the middle disc is connected in parallel with the two outer discs in series as shown in Fig. 1. Here, the small dots indicate the polarity of the piezo-electric discs. Thus, when an electric field is applied, the middle disc moves in opposition to the two outer discs. With this construction, the gap between the discs is field-free, and the liquid is subjected to a purely mechanical perturbation.

The capacitance of each disc depends on its strain state, so if the liquid partially clamps the disc (thus hindering its motion), the measured capacitance is lower than that of freely moving discs. By measurement of the electrical capacitance of the PSG, one can obtain the stiffness of the liquid in contact with the disc. In other words, one converts the electric impedance into the shear modulus knowing the exact relationship between the two.

The elasto-electric compliance matrix describes the relation between the components of the stress $\sigma_{ij}$ and strain $\epsilon_{ij}$ tensors to the electrical field of the piezo-electric material.[2] The equations describing an axially polarized ceramic can be split into four independent parts, the relevant of which can be reduced to the following:[2]

$$\begin{pmatrix} \sigma_{rr} \\ \sigma_{\phi\phi} \\ D_z \end{pmatrix} = \begin{pmatrix} c_{11} & c_{12} & -e_{13} \\ c_{12} & c_{11} & -e_{13} \\ e_{13} & e_{13} & \varepsilon_{33}^S \end{pmatrix} \begin{pmatrix} \epsilon_{rr} \\ \epsilon_{\phi\phi} \\ E_z \end{pmatrix}, \tag{A1}$$

where $E_z$ is the $z$-component of the electric field, $D_z$ is the displacement field, $c_{11}$ and $c_{12}$ are elastic constants of the ceramic, $\epsilon_{33}^S$ is the dielectric constant, and $e_{13}$ is a piezo-electric

constant. All of these quantities are weakly frequency dependent.

The measured capacitance $C_m$ of the disc can be found by integrating the charge density $D_z$ to find the total charge $Q$ and dividing by the voltage $U$,

$$C_m = \frac{Q}{U} = \frac{\int_0^{r_0} 2\pi r D_z(r)\, dr}{\xi E_z}, \tag{A2}$$

where $\xi$ is the thickness of the disc. $D_z$ depends both on the strain state and the applied electrical field $E_z$. Evaluating this integral, it is found[2] that the capacitance is a function of the radial displacement at the edge of the disc $u_r(r_0)$,

$$C_m = Au_r(r_0) + B, \tag{A3}$$

where $A$ and $B$ are known constants.

It remains to determine the displacement at the edge of the disc $u_r(r_0)$ as a function of rigidity of the liquid. The displacement $u_r$ is found by solving the radial equation of motion, which reduces to[2]

$$c_{11}(r^2(u_r'') + u_r' - u_r) - \sigma_l \frac{r^2}{\xi} = -\omega^2 r^2 \rho u_r, \tag{A4}$$

where the prime indicates the derivative with respect to $r$, and $\sigma_l$ is the tangential stress that the liquid exerts on the disc. $\sigma_l$ is by definition proportional to the shear modulus of the liquid $\sigma_l = G(\omega)u_r/d$, where $d$ is the thickness of the liquid layer (or equivalently 1/3 of the distance between the discs).

Figure 13 shows the measured capacitance of the empty (black trace) and liquid-filled (blue trace) PSG. At high temperatures, there is no influence from the liquid at these frequencies and the two spectra are identical. The spikes in the spectrum are mechanical resonances of the discs. At lower temperatures, the shear modulus of the liquid increases and partially clamps the discs in the quasi-static region. This is observed as a drop in the capacitance below the first resonances. The liquid also influences the position of the higher harmonics as compared with the spectrum of the empty device. At frequencies below the first resonances, which we refer to as the quasi-static region, the shear modulus is found by the described inversion procedure.[2] The inverted data, i.e., the complex shear modulus as function of frequency can be seen in Fig. 3.

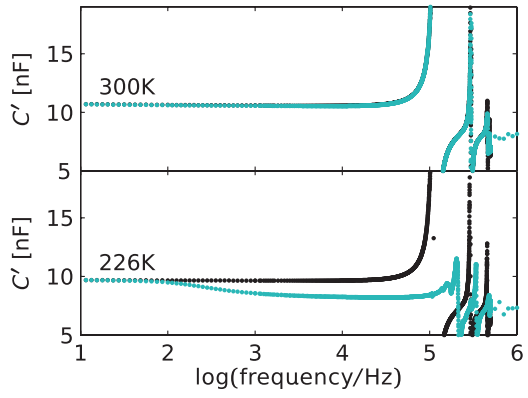


FIG. 13. Raw data of the empty (black) and liquid-filled (blue) PSG at two different temperatures. At 300 K the presence of the liquid does not affect the signal because the liquid is quite fluid. At 226 K the liquid partial clamps the discs, which is manifested as a drop in capacitance in the quasi-static region and a shift of the resonances in the high-frequency region.

## APPENDIX B: MODELING THE PBG

If the thickness of the ceramic shell is assumed to be vanishing, one can model the bulk transducer by an electrical circuit. The model presented here is equivalent to the model of Christensen and Olsen,[1] even though they did not explicitly state the electrical circuit model for the PBG.

Figure 14 shows the electrical equivalent circuit of the piezo-ceramic shell that illustrates how we model the bulk transducer. The model has an electrical side that models the electrical input, here the capacitor models the electrodes of the shell and the dielectric properties of the ceramic. On the right-hand side, the mechanical properties of the ceramic are modelled. The conversion from electrical to mechanical energy happens through the transducer element. On the mechanical side, the capacitor models the elastic properties of the ceramic, the inductance models the mass (or inertance), and the resistor models the friction. Seen from the electrical side, the mechanical and electrical sides are connected in parallel. This results from a consideration of limits: at high frequencies where the ceramic is mechanically clamped there is still charge on the electrodes, thus the electrical capacitor cannot be in series with the mechanical side. The mechanical elements are connected in series because they are all subjected to the same volume change (the mechanical equivalent of charge).

With this electrical circuit established, it is easy to construct the mathematical expression that gives the measured capacitance for the empty transducer,

$$C_m^{\text{emp}}(\omega) = C_1 + T^2 \frac{1}{\frac{1}{C_2} + i\omega R - \omega^2 L}. \tag{B1}$$

We rewrite this in terms of more familiar and recognizable quantities as follows:

$$C_m^{\text{emp}}(\omega) = C_{\text{cl}} + \frac{C_{\text{fr}} - C_{\text{cl}}}{1 + i\frac{\omega}{\omega_0}\frac{1}{Q} - \left(\frac{\omega}{\omega_0}\right)^2}, \tag{B2}$$

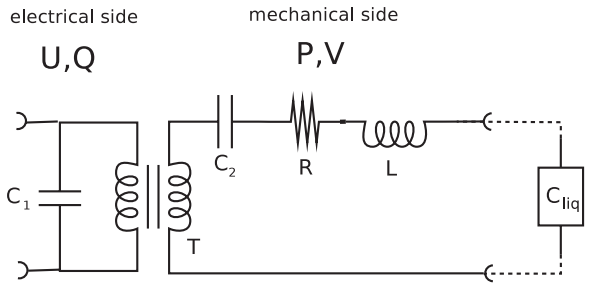


FIG. 14. Model of the bulk transducer. The electrical part (the capacitor) models the electrodes on the piezo-ceramic shell, the transformer models the conversion from electric displacement (charge) to deformation (volume change) in the ceramic. The RCL series models the mechanical properties of the PZ shell itself. For the empty tranducer, the mechanical port is short-circuited (i.e., free to move), while a filled transducer adds an extra element (box) in series with the RCL series.

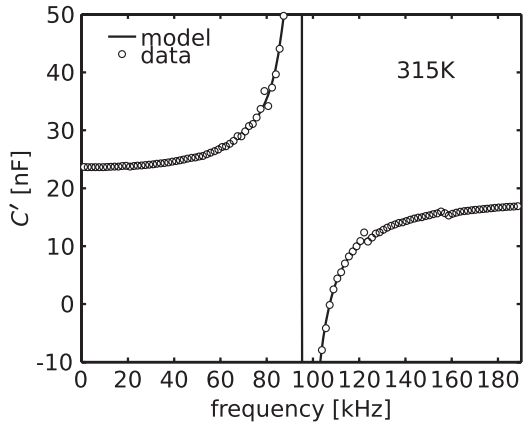


FIG. 15. Spectrum of the empty bulk transducer at 315 K (circles) and the fitted model (full line). The model fits the data well. The "jitter" on the high frequency side of the resonance is probably extra resonance modes reflecting a slightly imperfect spherical geometry.

where $C_{cl} = C_1$ is the "clamped" capacitance ($\omega \to \infty$), $C_{fr} = C_1 + T^2 C_2$ is the "free" capacitance ($\omega \to 0$), $\omega_0 = \sqrt{1/LC_2}$ is the resonance frequency, and $Q = (1/R)\sqrt{L/C_2}$ is the quality factor.

From fitting this expression to the spectrum of the empty capacitor, we can determine the four quantities $C_{\rm fr}$, $C_{\rm cl}$, $Q$, and $\omega_0$. An example of the fit is shown in Fig. 15. The model (full line) fits the data (circles) very well.

According to our model, the measured capacitance for the liquid-filled transducer is

$$C_m^{\rm liq}(\omega) = C_{\rm cl} + \frac{C_{\rm fr} - C_{\rm cl}}{1 + i\frac{\omega}{\omega_0}\frac{1}{Q} - \left(\frac{\omega}{\omega_0}\right)^2 + \frac{C_2}{C_{\rm liq}}}. \tag{B3}$$

This means that in order to de-convolve the stiffness of the liquid one must determine $C_2$. With only four fitted parameters and five in the model we need to determine the fifth by another method. Fortunately, the inductance $L$ can be determined by measuring dimension and weight of the transducer. $L$ is the constant of proportionality between the (generalized) voltage and charge acceleration, which expressed in mechanical variables is the pressure difference $\delta p$ and volume acceleration $\delta\ddot{V}$,

$$\delta p = L\delta\ddot{V}. \tag{B4}$$

$L$ is a constant of the specific bulk transducer and should be temperature independent. This means that we only need to determine this number once for each bulk transducer.

Expressing $\delta p$ as a force per unit area, this force will be given by mass times acceleration, i.e., $\delta p = m\ddot{u}_r/A$. Since the displacement is small, we can approximate the change in volume by $\delta V \approx A u_r$. In summary, we get

$$L = \frac{\delta p}{\delta\ddot{V}} \approx \frac{\ddot{u}_r m/A}{A\ddot{u}_r} = \frac{m}{A^2}. \tag{B5}$$

An estimate of the mass of the piezo-ceramic shell can be found by weighing the bulk transducer and subtracting the mass of the attached reservoir. For the surface area we need to be a little more careful: the model of the PBG assumes vanishing thickness of PZ shell, but this is of course just an approximation. Thus, we should find an "effective" surface area, which will be between the outer and inner surface of the shell. Assuming an average of the two gives a good estimate of $L$.

For simplicity, we define the dimensionless measured capacitance,

$$F(\omega) = \frac{C_m^{\rm liq}(\omega) - C_{\rm cl}}{C_{\rm fr} - C_{\rm cl}}. \tag{B6}$$

Finally, the complex stiffness of the liquid (defined as $S = \delta p/\delta V$) can be expressed in terms of the four fitted parameters and $L$,

$$S_{\rm liq}(\omega) = \frac{1}{C_{\rm liq}(\omega)} = L\omega_0^2\left\{\frac{1}{F} - 1 - i\frac{\omega}{\omega_0}\frac{1}{Q} + \left(\frac{\omega}{\omega_0}\right)^2\right\}. \tag{B7}$$

The bulk modulus $K$ is then found as $K = VS$, where $V$ is the volume of the liquid (inner volume of the shell).

## APPENDIX C: MODELLING THE FLOW THROUGH THE HOLE

At high frequencies the hole is essentially blocked because the liquid does not have time to flow in and out during one frequency cycle. In that case we can consider the liquid inside as a perfect spherical "ball."

At high temperatures (far above $T_g$), the liquid flowing in and out of the hole is a Helmholtz resonator, but as temperature is lowered, this resonance gets damped due to the increase in viscosity. When the resonance gets critically damped, it moves down in frequency upon further cooling. In Fig. 16, this is shown for DC704.

At low enough frequencies the liquid is able to flow in and out of the hole. This flow can be assumed to be inertia free since it is extremely slow, and it can thus be modelled as a Poiseuille flow. A Poiseuille flow describes the laminar flow of fluid in a pipe with radius $a$ and length $l$ ($l > a$) with a no-slip boundary condition at the walls of the pipe.

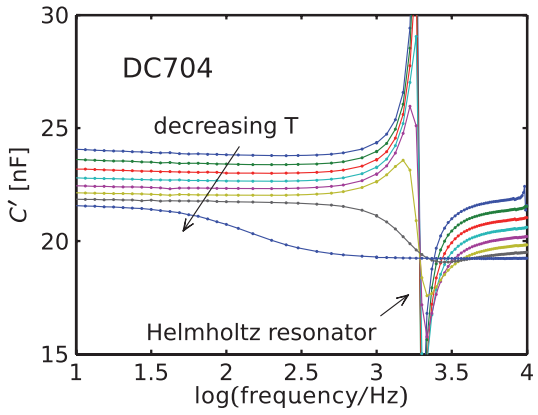


FIG. 16. The measured capacitance of DC704. At high temperatures the liquid flowing in and out of the hole gives rise to a resonance. When the temperature is lowered this resonance gets damped because the viscosity of the liquid increases. Finally, when the resonance is critically damped, it moves down in frequency as temperature is lowered.

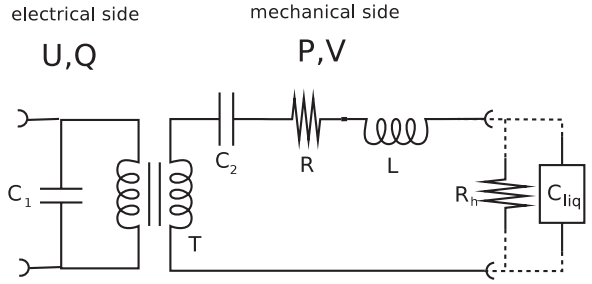


FIG. 17. The electrical network model of the PBG of Fig. 14 with an extra element added to model the flow through the hole.

For a Poiseuille flow the volume flow is given by the following expression (for a derivation see, e.g., Ref. 34):

$$\dot{V} = \frac{\pi a^4 \delta p}{8 \eta_G l}, \tag{C1}$$

where $\eta_G$ is the (shear) viscosity, $\dot{V}$ is the volume flow-rate, and $\delta p$ is the pressure difference across the "pipe."

In the framework of the electrical network model, the flow can be added as a resistor in parallel with the liquid, since it is subjected to the same pressure difference (we ignore the mass since the flow is so slow that inertial effects are vanishing). This is illustrated in Fig. 17. From Eq. (C1), we obtain an expression for this resistor which is basically the shear viscosity times a geometric factor

$$R_P = \frac{\delta p}{\dot{V}} = \frac{8l}{\pi a^4} \eta_G \,, \tag{C2}$$

which we use later.

We determine $R_P$ from the mechanical impedance of the measured signal ($Z = S/(i\omega) = 1/i\omega C_m$). The impedance of the signal coming from the liquid is given by

$$Z = \frac{1}{1/R_P + i\omega C_{\text{liq}}} = R_P \frac{1}{1 + i\omega\tau}, \tag{C3}$$

where $\tau = R_P C_{\text{liq}}$. The flow through the hole is thus described by a pure exponential, and plotting the imaginary part versus the real part will describe a semi-circle with $R_P$ as the low frequency foot point. An example of this is shown in the main text in Fig. 10, where the red circles are data points and the black solid line shows the exponential fit. Because the data trace out a semi-circle with the centre on the real axis, $R_P$ can also be found as twice the value of $Z'$ at the top point,

$$R_P = 2Z'(\omega_{\max}), \tag{C4}$$

which is easy to determine. In Fig. 18, we show this for a range of different temperatures. Here, both the real and imaginary axes are plotted logarithmically to contain all data in one plot and thus it is not obvious to the eye that the data trace out semicircles. The cross marks the peak position for each temperature which is then proportional to the shear viscosity.

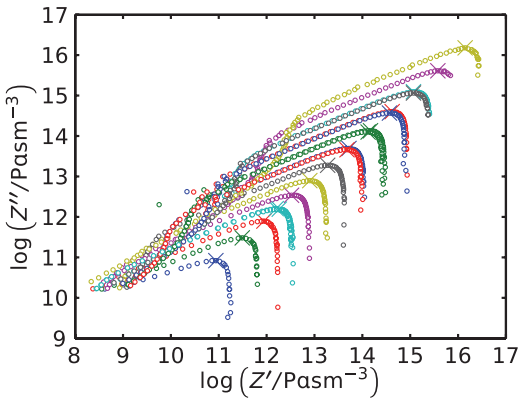


FIG. 18. Determining the shear viscosity from the Helmholtz mode. The flow resistance $R_P$ can be determined by the high-frequency limit of the mechanical impedance, $Z = VS/i\omega$. Since the Helmholtz mode is Debye-like, however, the $Z$ traces out a semi-circle (see Fig. 10) and we only need to know the peak position to determine $R$. Here, we used a double-log plot to fit all data in the same window, which of course distorts the circular shape.


[1] T. Christensen and N. B. Olsen, Phys. Rev. B **49**, 15396 (1994).
[2] T. Christensen and N. B. Olsen, Rev. Sci. Instrum. **66**, 5019 (1995).
[3] C. Klieber, T. Hecksher, T. Pezeril, D. H. Torchinsky, J. C. Dyre, and K. A. Nelson, J. Chem. Phys. **138**, 12A544 (2013).
[4] T. Christensen and N. B. Olsen, J. Non-Cryst. Solids **172-174**, 362 (1994).
[5] Y. Meng and S. L. Simon, J. Polym. Sci., Part B: Polym. Phys. **45**, 3375 (2007).
[6] R. S. Marvin, R. Aldrich, and H. S. Sack, J. Appl. Phys. **25**, 1213 (1954).
[7] E. Morita, R. Kono, and H. Yoshizak, Jpn. J. Appl. Phys. **7**, 451 (1968).
[8] A. R. Dexter and A. J. Matheson, J. Chem. Phys. **54**, 3463 (1971).
[9] V. A. Solovyev, Y. S. Manucharov, and I. Alig, Acta Polym. **40**, 513 (1989).
[10] I. Alig, F. Stieber, A. D. Bakhramov, Y. S. Manucharov, S. A. Manucharova, and V. A. Solovyev, Polymer **31**, 877 (1990).
[11] M. Schulz and I. Alig, J. Chem. Phys. **97**, 2772 (1992).
[12] A. F. Yee and M. T. Takemori, J. Polym. Sci., Polym. Phys. Ed. **20**, 205 (1982).
[13] B. Igarashi, T. Christensen, E. H. Larsen, N. B. Olsen, I. H. Pedersen, T. Rasmussen, and J. C. Dyre, Rev. Sci. Instrum. **79**, 045105 (2008).
[14] B. Igarashi, T. Christensen, E. H. Larsen, N. B. Olsen, I. H. Pedersen, T. Rasmussen, and J. C. Dyre, Rev. Sci. Instrum. **79**, 045106 (2008).
[15] T. Hecksher, "Relaxation in supercooled liquids," Ph.D. dissertation (Roskilde University, 2010).
[16] B. Jakobsen, K. Niss, and N. B. Olsen, J. Chem. Phys. **123**, 234511 (2005).
[17] N. B. Olsen, T. Christensen, and J. C. Dyre, Phys. Rev. Lett. **86**, 1271 (2001).
[18] L.-M. Wang and R. Richert, Phys. Rev. B **76**, 064201 (2007).
[19] A. I. Nielsen, B. Jakobsen, K. Niss, N. B. Olsen, R. Richert, and J. C. Dyre, J. Chem. Phys. **130**, 154508 (2009).
[20] M. T. Cicerone and M. D. Ediger, J. Chem. Phys. **104**, 7210 (1996).
[21] L. M. Wang and R. Richert, J. Chem. Phys. **121**, 11170 (2004).
[22] B. Jakobsen, T. Hecksher, T. Christensen, N. B. Olsen, J. C. Dyre, and K. Niss, J. Chem. Phys. **136**, 081102 (2012).
[23] R. Zorn, F. I. Mopsik, G. B. McKenna, L. Willner, and D. Richter, J. Chem. Phys. **107**, 3645 (1997).
[24] R. D. Deegan, R. L. Leheny, N. Menon, S. R. Nagel, and D. C. Venerus, J. Phys. Chem. B **103**, 4066 (1999).
[25] W. Suchanski, S. Jurga, T. Pakula, M. Paluch, and J. Ziolo, J. Phys.: Condens. Matter **12**, 9551 (2000).
[26] C. Dreyfus, S. Murugavel, R. Gupta, M. Massot, R. M. Pick, and H. Z. Cummins, Philos. Mag. B **82**, 263 (2002).
[27] R. Kono, T. A. Litovitz, and G. E. McDuffe, J. Chem. Phys. **45**, 1790 (1966).
[28] E. Rössler and P. Eiermann, J. Chem. Phys. **100**, 5237 (1994).
[29] J. C. Hooker and J. M. Torkelson, Macromolecules **28**, 7683 (1995).
[30] K. Schröter and E. Donth, J. Non-Cryst. Solids **307–310**, 270 (2002).
[31] P. K. Dixon, L. Wu, S. R. Nagel, B. D. Williams, and J. P. Carini, Phys. Rev. Lett. **65**, 1108 (1990).
[32] B. Jakobsen and K. Niss, "Dielectric and shear mechanical relaxation in glass forming liquids," Master's thesis, Roskilde University, 2003.
[33] G. Harrison, *The Dynamic Properties of Supercooled Liquids* (Academic, 1976).
[34] A. L. Fetter and J. D. Walecka, *Theoretical Mechanics of Particles and Continua* (Dover, 2003).
[35] The data can be obtained from the "Glass and Time: Data repository," see http://glass.ruc.dk/data.